

# Extensive Biotransformation Profiling of AZD8205, an Anti-B7-H4 Antibody-Drug Conjugate, Elucidates Pathways Underlying its Stability *In Vivo*

Yue Huang<sup>1\*</sup>, Hui Yin Tan<sup>1</sup>, Jiaqi Yuan<sup>1</sup>, Ruipeng Mu<sup>1</sup>, Junyan Yang<sup>1</sup>, Kathryn Ball<sup>2</sup>, Balakumar Vijayakrishnan<sup>3</sup>, Luke Masterson<sup>3</sup>, Krista Kinneer<sup>4</sup>, Nadia Luheshi<sup>5</sup>, Meina Liang<sup>1</sup>, Anton I. Rosenbaum<sup>1\*</sup>

<sup>1</sup>Integrated Bioanalysis, Clinical Pharmacology and Safety Sciences, R&D, AstraZeneca, South San Francisco, CA 94080, USA

<sup>2</sup>Clinical Pharmacology and Quantitative Pharmacology, Clinical Pharmacology and Safety Sciences, R&D, AstraZeneca, Cambridge CB21 6GH United Kingdom

<sup>3</sup>TTD, Oncology R&D, AstraZeneca, London E1 2AX, United Kingdom

<sup>4</sup>Translational Medicine, Oncology R&D, AstraZeneca, Gaithersburg, MD 20878, USA

<sup>5</sup> Oncology R&D, AstraZeneca, Cambridge CB2 8PA, United Kingdom

\*Corresponding Authors

Yue Huang - 121 Oyster Point Blvd, South San Francisco, CA 94080, USA; Tel: +1-650-481-6801; E-mail: [yhuang@revmed.com](mailto:yhuang@revmed.com)

Anton I. Rosenbaum - 121 Oyster Point Blvd, South San Francisco, CA 94080, USA; Tel: +1-650-379-3099; E-mail: [anton.rosenbaum@astrazeneca.com](mailto:anton.rosenbaum@astrazeneca.com)

## Abstract

What happens to macromolecules *in vivo*? What drives structure-activity relationship and *in vivo* stability for antibody-drug conjugates (ADCs)? These interrelated questions are increasingly relevant due to the re-emerging importance of ADCs as an impactful therapeutic modality and the gaps that exist in our understanding of ADC structural determinants that underlie ADC *in vivo* stability. Complex macromolecules, such as ADCs may undergo changes *in vivo* due to their intricate structure as biotransformations may occur on the linker, the payload and/or at the modified conjugation site. Furthermore, dissection of ADC metabolism presents a substantial analytical challenge due to the difficulty in identification or quantification of minor changes on a large macromolecule. We employed immunocapture-LCMS methods to evaluate *in vivo* changes in drug-antibody ratio (DAR) profile in four different lead ADCs. This comprehensive characterization revealed that a critical structural determinant contributing to ADC design was the selection of the linker as the competition between the retro-Michael deconjugation and thio-succinimide hydrolysis reactions resulted in superb conjugation stability *in vivo*. These data, in conjunction with additional factors, informed the selection of AZD8205, a B7-H4-directed cysteine-conjugated ADC bearing a novel topoisomerase I inhibitor payload, with durable DAR, currently being studied in the clinic for the potential treatment of solid malignancies (NCT05123482). These results highlight the relevance of studying macromolecule biotransformation and elucidating the ADC structure-*in vivo* stability relationship. The comprehensive nature of this work increases confidence in our

understanding of these processes. We hope this analytical approach can inform future development of bioconjugate drug candidates.

## Introduction

Over the past decades structural characterization of macromolecules *in vitro* has advanced significantly. A plethora of techniques have been employed to characterize the structure of a protein macromolecule primary sequence as well as secondary and tertiary structure at atomic and sub-atomic resolution. Advanced techniques have been applied to characterize molecular dynamics of molecules<sup>1,2</sup> and recent advances have focused on characterization of macromolecular complexes and non-covalent interactions<sup>3,4</sup>. In the case of small molecules, the structural characterization *in vitro* has been extended to the *in vivo* realm under the auspices of biotransformation analyses. Decades of research into biotransformation of small molecule xenobiotics enriched our understanding of such processes. However, characterization of changes to *protein* macromolecule structure *in vitro* as well *in vivo*, i. e. biotransformation, is an emerging area of scientific inquiry<sup>5,6</sup>. The main biotransformation pathway for traditional protein therapeutics such as monoclonal antibodies (Mabs) usually involves straightforward proteolysis<sup>7</sup>. Therefore, recent work in macromolecule biotransformation has focused primarily on characterization of complex biotherapeutics such as antibody-drug conjugates (ADCs)<sup>8-10</sup>.

ADCs combine the high specificity of monoclonal antibodies and potent cytotoxic drugs connected by a cleavable or non-cleavable linker for targeted drug payload delivery<sup>11</sup>. Presently, 15 ADCs have obtained approval from Food and Drug Administration (FDA) or European Medicines Agency (EMA)<sup>12,13</sup>. ADCs are typically designed to stay intact while in circulation and release their drug payload upon target-mediated internalization into tumor cells, maximizing therapeutic index (TI). The linker design plays a major role in modulating the timing and location of drug release<sup>14</sup>. However, biotransformation of ADCs, such as payload deconjugation or modification to the antibody, drug or linker can impact their *in vivo* stability<sup>7,15</sup>. Hence, in-depth characterization of ADC biotransformations would aid in their chemical optimization influencing *in vivo* stability.

Bioanalytical strategies for the quantification and characterization of novel bioconjugate therapeutics have been thoroughly discussed over the past several years<sup>6,16</sup>. Typical approaches for ADC quantification in support of pharmacokinetic assessments entail monitoring surrogate analytes (peptides/payloads) via a targeted bottom-up approach. Therefore, information on the biotransformation can be lost without *a priori* knowledge. High resolution accurate mass spectrometry (HRMS) based intact analysis of ADCs coupled with chromatographic separation is a powerful and robust tool for the identification of novel biotransformation species. Recent advances in the field of HRMS in addition to more efficient ionization of macromolecules enable the progress of analyzing intact biotherapeutics such as mAbs and ADCs<sup>17-20</sup>. However, other approaches such as CE, HIC and SEC coupled with MS have been employed as well. Han et al.<sup>16</sup> reported case studies with CE-MS applied to protein biotransformation analysis. He et al.<sup>17</sup> pioneered in ADC biotransformation with RPLC-MS approaches. Additional applications of HIC-MS<sup>18</sup> and SEC-MS<sup>19</sup> suggest that alternative approaches can be explored for structural analyses of ADCs.

AZD8205 is a B7-H4-targeted ADC utilizing a novel topoisomerase I linker-payload<sup>21</sup> (**Figure 1**) being studied in the clinic for the treatment of biliary tract, breast, ovarian or endometrial cancers (NCT05123482)<sup>22,23</sup>. As part of the structure-activity relationship (SAR) optimization of AZD8205 we examined 4 different linkers to enable the conjugation of the topoisomerase I payload (TOP1i

AZ14170132)<sup>22</sup>. The payload was covalently conjugated to native interchain cysteines of an anti-B7-H4 antibody via either a caproyl or propionyl-PEG8 spacer to a Val-Ala (VA) or Gly-Gly-Phe-Gly (GGFG) peptide linker (**Figure 1**), resulting in four distinct anti-B7-H4 ADCs, each with an approximate drug-to-antibody ratio (DAR) of 8. To characterize AZD8205 pharmacokinetics and biotransformation using both *in vitro* incubation and *in vivo* plasma samples in mice dosed with AZD8205, we employed intact and bottom-up approaches. Herein, we describe comprehensive characterization of pharmacokinetics and biotransformation of an ADC from both *in vitro* and *in vivo* samples, employing orthogonal approaches providing complementary information. The findings confirmed durable structural and conjugation stability of AZD8205 among the 4 linker designs evaluated.

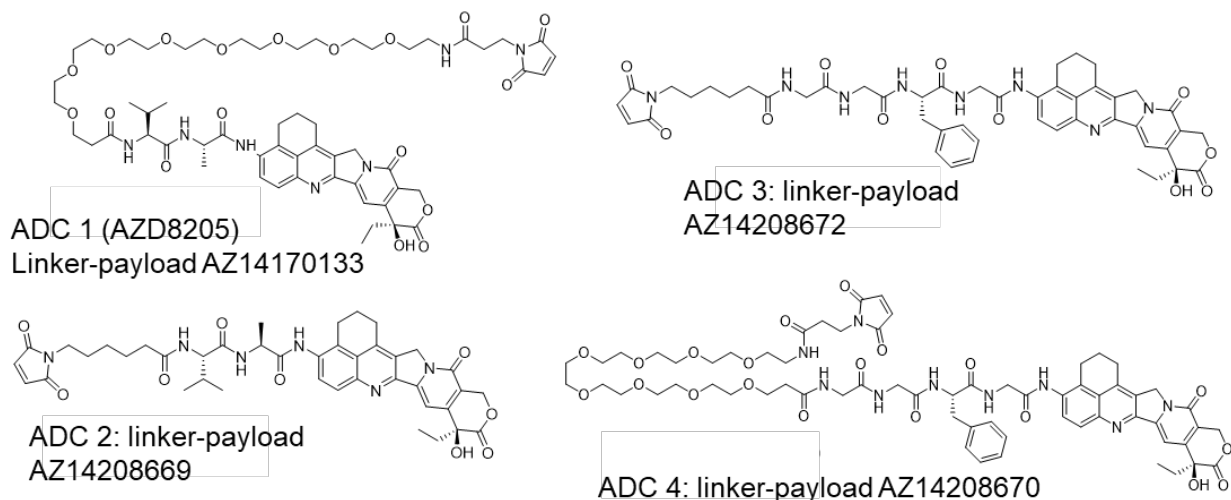


**Figure 1.** Schematic representation of the linker-payload structures evaluated.

## Materials and Methods

### Materials and Reagents

All ADCs, payload and stable isotope labeled payload, anti-idiotype and anti-payload antibodies used were provided by AstraZeneca (Gaithersburg, MD). Anti hu-Fc capture antibody was purchased from Bethyl. Peptide internal standards were custom synthesized by Vivitide. The pooled plasma was purchased from BioIVT. The SMART IA magnetic beads, tris(hydroxymethyl)aminomethane (Tris) buffer, Phosphate-buffered saline (PBS), Zeba 7K MWCO spin column, formic acid (FA), trifluoroacetic acid (TFA), and sulfo-NHS biotin were all purchased from Thermo Scientific. Bovine serum albumin and papain were purchased from Sigma-Aldrich. The chromatographic columns (BEH C18 and BioResolve) were purchased from Waters. All other reagents were purchased from VWR.

### LC-MRM Method for Quantification of Total Antibody, Intact Antibody and ADC Concentration

Calibration curve standards and quality control samples were prepared in blank pooled CD-1 mouse plasma using reference standard AZD8205. Calibration range was 0.100-15.0  $\mu\text{g/mL}$ . 50  $\mu\text{L}$  of AZD8205 sample was then enriched by immunoaffinity capture using 30  $\mu\text{L}$  SMART IA streptavidin beads conjugated to 3  $\mu\text{g}$  biotinylated anti human-Fc with approximately 2 h incubation at ambient temperature. After separating the beads from supernatant and extensive washing of the beads, SMART IA

digestion buffer with stable isotope-labeled internal standard was added to beads for tryptic digestion at 70 °C for 2 h. After trypsin digestion, one fraction of the supernatant was used for total antibody and intact antibody assay. The other fraction was further digested using 0.5 mg/mL papain (overnight at 37 °C) to release AZ14170132 for ADC assay. The characteristic peptides were quantified as surrogate analytes for the total antibody (heavy chain peptide - GLEWIGEINHSGSTSYNPSLK) and intact antibody (light chain peptide – NDVGWYQQKPGK) concentrations and the released AZ14170132 served as the surrogate analyte for the ADC concentration. Internal standards used were stable isotope labeled peptides (terminal lysine  $^{13}\text{C}_6$ ,  $^{15}\text{N}_2$ ) and payload ( $^2\text{H}_5$ ). The ADCs were immunocaptured using the heavy chain. Total antibody assay monitors heavy chain peptide whereas intact antibody monitors light chain peptide. The presence of light chain confirms that the antibody is intact since there is no interchain disulfide bond in these DAR8 ADCs. The ADC concentration included all species of biotransformed molecules with payload in a DAR-sensitive manner, regardless of linker biotransformations. All three assays were analyzed on the SCIEX Triple Quadrupole 6500+ mass spectrometer coupled with a Shimadzu liquid chromatography system. Chromatographic separation was performed using Waters ACQUITY UPLC BEH C18 Column (PN186002350). Mobile phases were A: 0.1 % formic acid in water and B: 0.1 % formic acid in acetonitrile with flow rate of 0.5 mL/min at 60°C. Data were acquired and analyzed with Analyst (v1.7) and MultiQuant (v3.0.3863) software, respectively.

## Intact LC-HRMS Profiling of Biotransformation Species

An intact LC-HRMS assay was developed to characterize ADC biotransformation species from *in vitro* and *in vivo* samples. This method allows a more specific identification of various biotransformation species as well as unbiased quantification. For each sample, the ADC concentration was first measured with the LBA-LC-MRM assay. Plasma concentrations were then adjusted to achieve 8.3 µg/mL ADC with a 120 µL aliquot enabling capture of 1 µg ADC. For certain samples with low concentrations where 1 µg of ADC was not achievable, the maximum volume of original plasma available was used (**Table S1**) in capture step. The plasma sample and 75 µL SMART IA magnetic beads conjugated with 12.5 µg biotinylated anti-human Fc (a-HuFc) or anti-payload antibody were incubated for approximately 30 min at ambient temperature to capture the ADC and its biotransformed species. After the removal of the supernatant following the capture step, the beads were then washed twice with PBS and then twice with water (250 µL each wash step). Finally, the ADC and biotransformed species were eluted off the beads by incubating the beads for 5 min with 45 µL 1% FA in water with cytochrome C. The samples were not deglycosylated or reduced to preserve the maximal information for identification of biotransformation species. The eluted samples were injected onto Shimadzu Nexera LC. The separation was performed on a Waters BioResolve RP mAb polyphenyl column (PN186009017) with 1% FA, 0.01% TFA in water/ACN as mobile phases with flow rate of 0.5 mL/min at 80°C (example chromatogram in **Figure 2A**). Under the denaturing conditions of reversed phase liquid chromatography, DAR8 ADC light chain and heavy chain would separate due to the replacement of inter-chain disulfide bonds with linker-payloads. A shallow gradient was applied in the reversed phase separation to resolve the various species and the major parent molecule. After LC, the separated species were then ionized and acquired in full scan mode with either SCIEX 6600 Triple TOF or 7600 Zeno TOF system.

## Deconvolution, identification and quantification of Intact LC-HRMS data

The mass spectra were deconvoluted using a research version PeakView (version number: 1.2.2.0) with a sliding window method (**Figure S1**). This approach converts every 3 spectra within m/z-time domain to deconvoluted spectra in mass-time domain. This preserves chromatographic features such as retention time. The automated method treated all data in a consistent manner, eliminating the analyst bias in peak selection. This deconvolution method also eliminated the potential impact from neighboring main peak with high signal intensity on the smaller biotransformed peaks with lesser signal intensity. The mass-time information was then used to manually identify the biotransformed species structures. To quantify the relative abundance of the various biotransformed species, the mass-time chromatograms were analyzed with MultiQuant software using automatic peak integration (MQ4) at the theoretical mass with +/- 50 ppm as the extraction range. Pre-spiked cytochrome C was used to monitor run performance. Extracted peak area of each species was normalized with injected ADC mass for comparison between timepoints. For relative quantification of biotransformation species (% species) at each timepoint, the percentage was calculated by dividing the sum peak area of a class of species that shared a common feature (e.g. all heavy chain species with G0F) by the sum peak area of all biotransformation species in that class, including parent species (e.g. all heavy chain species).

## Results

### Characterization of Pharmacokinetics with LBA-LC-MRM

The most common approach to understand macromolecule biotransformation is to use a surrogate analyte method and measure fragments from the region of interest to indirectly confirm the structural integrity of the macromolecule<sup>6,24</sup>. This was performed with LC-MRM methods for all ADCs in this study. The LBA-LC-MRM method was used to generate absolute quantitative results for the total Ab, intact Ab and ADC assay (**Figure S2, Table S2**). The data generated using the three methods resulted in overlapping concentration-time profiles for all four ADCs, suggesting that no significant de-conjugation was observed, and the protein scaffold remained stable. The differences in concentration-time profiles between the four ADCs with various linkers were not significant when characterized with LBA-LC-MRM assays, considering the 20% accuracy and precision acceptance criteria for the assays.

### Determination of *in vivo* Biotransformation Pathway Informs AZD8205 Lead Selection

To understand the impact different cleavable linkers would have on *in vivo* DAR stability we further examined ADC biotransformation pathways using LBA-LC-HRMS approach. In a DAR8 ADC where the interchain disulfide bonds were replaced by the payload conjugation, the light chain and the heavy chain are not covalently bonded and would separate under denaturing conditions of reversed phase chromatography. First, as shown in **Figure 2A**, the light chain and the heavy chain are well separated, with the associated biotransformed species of the light chain and heavy chain eluting in the area close to the parent light chain and the parent heavy chain. Second, to maximize the identification of the various biotransformed products and to facilitate quantification of these species in an unbiased manner, an automated deconvolution was performed with PeakView (research version), where each spectrum was deconvoluted separately and the m/z-time raw data were converted to a mass-time data. Third, manual identification of the major biotransformed species was performed based on the theoretical intact mass

difference between the parent peak and the biotransformed species (**Figure 2B, Table S3**). Then, extracted peak areas from the chromatograms were used for quantification (**Table S3**). Lastly, the chemical structures of these proposed biotransformed species (**Figure S3**) were further confirmed with LC-MS/MS with CID fragmentation using *in vitro* incubation samples that possessed the same biotransformation species (**Figures S4-S7**).

This approach unveiled various macromolecular biotransformed species from light chain (LC), heavy chain (HC) or half antibody, identified over the 12-day period post-dose of each ADC in Tg32 mice (**Figure 2, Table 1**). To perform relative quantification of complex biotransformation species, the various analytes were clustered based on the relevant characteristics to provide simplified metrics for profiling the *in vivo* mixture of ADC and its biotransformed species. There are two assumptions for relative characterization of this data set: 1) capture efficiency and ionization efficiency are reasonably comparable among species used for quantification; 2) data processing is performed uniformly for all species regardless of the signal intensity of the biotransformation species.

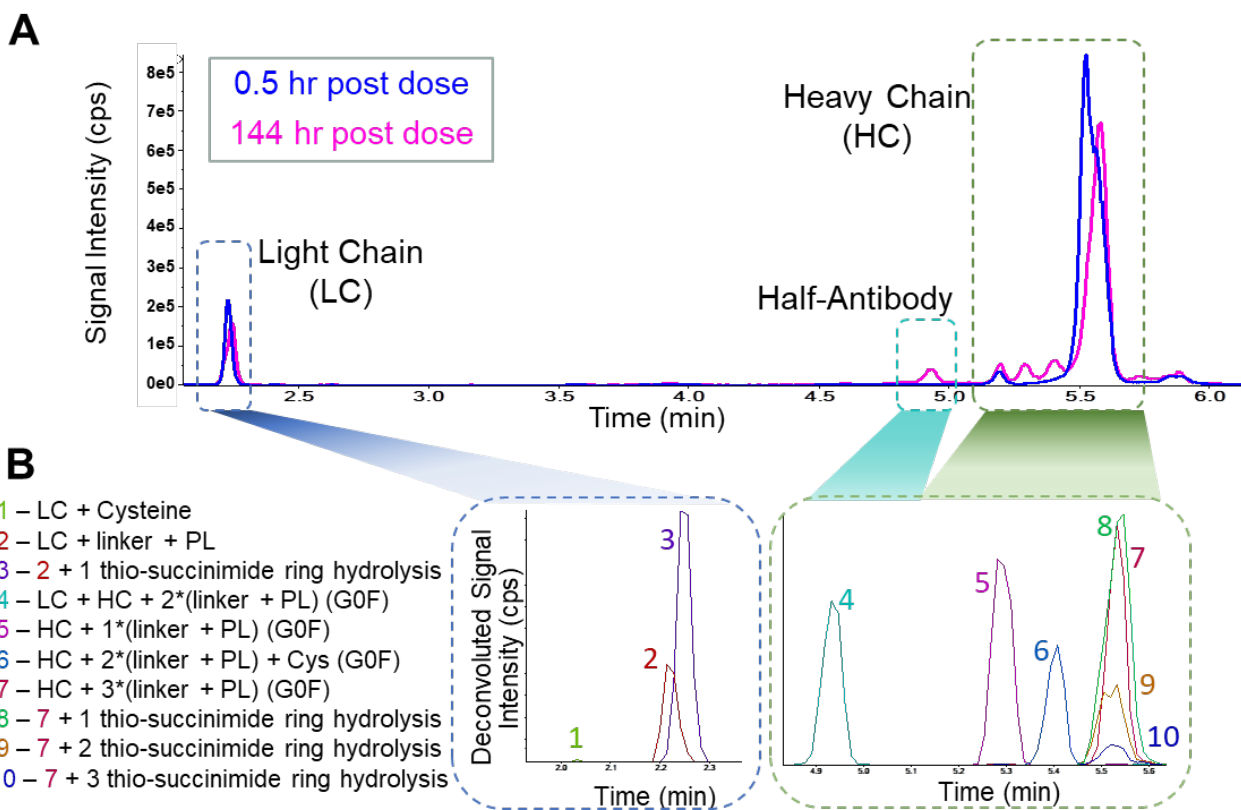


**Figure 2.** (A) Representative total ion chromatogram for the ADCs, 0.5 hr and 144 hr post dose in human FcRn mice. (B) Extracted ion chromatogram for selected major biotransformation species from deconvoluted data (mass-time) of peaks identified in A. LC: light chain, HC: heavy chain, PL: payload

**Table 1.** List of biotransformation species identified (LC: light chain, HC: heavy chain, PL: payload, Cys: cysteine)

Index	Monitoring Species	Index	Monitoring Species	Index	Monitoring Species
1	LC + 1PL	15	HC + 2PL + G0F + 2Water	29	HC + 3PL + G0F + 2Water
2	LC + 1PL + 1Water	16	HC + 2PL + G1F + 2Water	30	HC + 3PL + G1F + 2Water
3	LC	17	HC + 2PL + G0F + GSH	31	HC + 3PL + G0F + 3Water
4	LC + Cys	18	HC + 2PL + G1F + GSH	32	HC + 3PL + G1F + 3Water
5	HC + G0F	19	HC + 2PL + G0F + Cys	33	LC + HC + 2PL + G0F
6	HC + G1F	20	HC + 2PL + G1F + Cys	34	LC + HC + 2PL + G1F
7	HC + 1PL + G0F	21	HC + 2PL + G0F + 1Water + Cys	35	LC + HC + 2PL + G0F + 1Water
8	HC + 1PL + G1F	22	HC + 2PL + G1F + 1Water + Cys	36	LC + HC + 2PL + G1F + 1Water
9	HC + 1PL + G0F + 1Water	23	HC + 2PL + G0F + 2Water + Cys	37	LC + HC + 2PL + G0F + 2Water
10	HC + 1PL + G1F + 1Water	24	HC + 2PL + G1F + 2Water + Cys	38	LC + HC + 2PL + G1F + 2Water
11	HC + 2PL + G0F	25	HC + 3PL + G0F	39	Albumin
12	HC + 2PL + G1F	26	HC + 3PL + G1F	40	Albumin + Cys
13	HC + 2PL + G0F + 1Water	27	HC + 3PL + G0F + 1Water	41	Albumin + 1PL
14	HC + 2PL + G1F + 1Water	28	HC + 3PL + G1F + 1Water	42	Albumin + 1PL + 1Water

## Biotransformation Step 1: Hydrolysis or Deconjugation from the Conjugation Site

Thio-succinimide-conjugated payloads go through two competing biotransformation reactions: hydrolysis or deconjugation via retro-Michael reaction<sup>8</sup>. It was previously demonstrated that some linkers can partially deconjugate, resulting in a protein-partially cleaved payload structure<sup>9</sup>. Aside from the thio-succinimide ring hydrolysis, protein scaffold instability has also been reported<sup>24</sup> when the parent molecule has disrupted disulfide bonds. For ADC1 and ADC4 species with hydrolyzed thio-succinimide ring were the major biotransformation products on both the heavy chain and the light chain (**Figure 3A**). The retention time of these species did not alter significantly compared to the parent molecule. At 48 h post dose, the hydrolyzed forms replaced the original species and became the most abundant form of light chain for ADC1 and ADC4 (**Figure 3A**). For the heavy chain species, the hydrolysis happened gradually: generating partially hydrolyzed species first, then shifting to fully hydrolyzed species. The kinetics of the thio-succinimide hydrolysis is dependent on the chemistry of the linker: both ADC1 and ADC4 contain linkers with propionyl-PEG8 spacers between the amide and the thio-succinimide, resulting in faster hydrolysis rate compared to ADC2 and ADC3 (**Figure 3, S8**) that contain caproyl spacer only. The hydrolyzed species were also confirmed with LBA-LC-HRMS bottom-up identification, through both accurate mass MS1 as well as MS2 spectra (**Figure S4 Table S4**). The LC-conjugated linker-payload deconjugates less compared to the HC-conjugated ones for the four ADCs studied here, as observed by other researchers<sup>12, 24</sup>. In contrast to ADC1 and ADC4, for ADC 2 and ADC 3, the deconjugation on HC was observed as the major form especially for timepoints after 48 h (**Figure 3B**). Deconjugation results in lower DAR species. These species usually elute earlier compared to the parent molecule. For heavy chain

species, the parent heavy chain (with 3 payloads, HC-3PL) eluted around 5.6 min, with the biotransformed species eluting around 5.4 min (HC-2PL) and 5.3 min (HC-1PL), respectively (**Figure 2B**). Note that the degree of deconjugation on LC for all ADCs are consistently low (<0.4 %) compared to HC (**Figure 3B**).

Deconjugation of thio-succinimide-conjugated linker-payloads can result from two possible reactions: 1) retro-Michael elimination at the conjugation site, exposing the free thiol; and 2) step-wise linker cleavage, generating a series of antibody backbone species with partial linker moieties. In evaluating ADCs 1-4, only species consistent with reaction 1 deconjugation were observed. Therefore, the deconjugation and thio-succinimide hydrolysis processes for ADCs 1-4 are two competing reactions. There is a clear structure-stability relationship and *in vivo* biotransformation reaction preference observed between the ADCs with propionyl-PEG8 vs. caproyl spacer within the linker. This provides mechanistic basis for improved *in vivo* DAR stability for ADC1 (AZD8205) and ADC4 versus ADC2 and ADC3.

### Relative quantification from biotransformed species

The observed change in ADC DAR post-dose enables evaluation of ADC deconjugation over time. The DAR can be calculated by comparing the total Ab and ADC data from the absolute LC-MRM quantification (**Figure S9A**), or with the identified LC and HC species from relative intact LC-HRMS (**Figures 2, 3, S9B**). It is notable that both methods, to various extent, showed that ADC1 and 4 had a slower deconjugation rate over the time compared to ADC2 and 3. However, LC-HRMS assay was able to also characterize the structural differences in various species and kinetics of associated reactions.

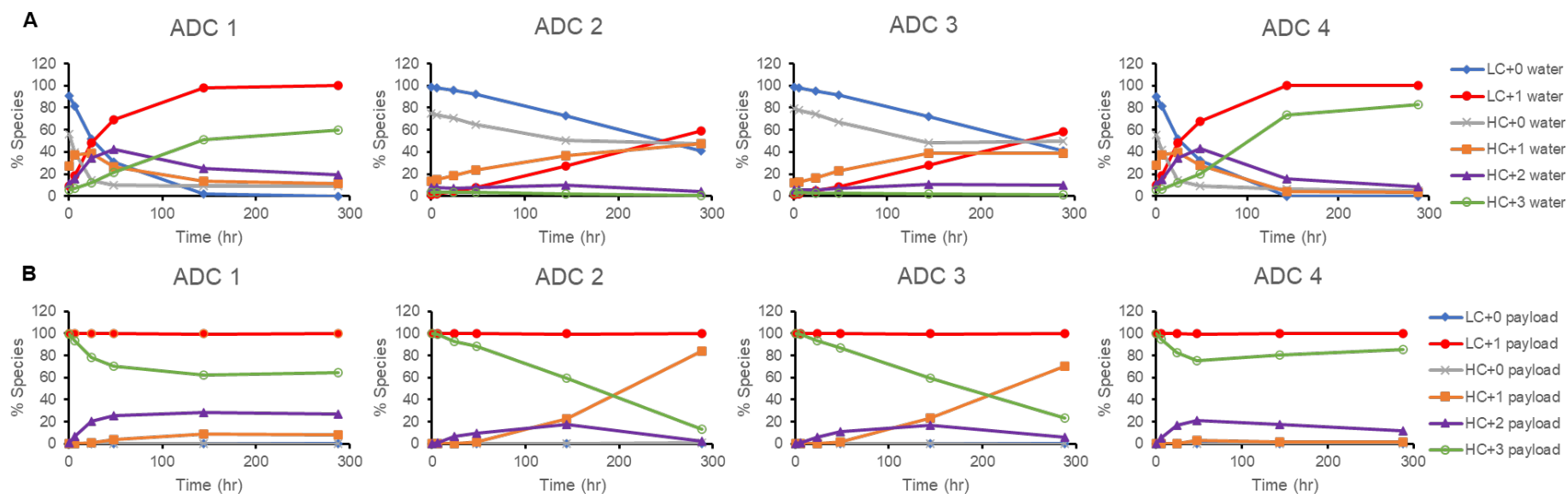


**Figure 3.** Changes in relative abundance of major biotransformation species for four ADC in mouse preclinical studies as function of time post-dose. (A) Thio-succinimide hydrolysis species. (B) Light and heavy chain species with varied numbers of conjugated payload(s). LC: light chain, HC: heavy chain. Representative MS1 spectra of these species can be found in **Figure S4**.

## Biotransformation Step 2: Reactions after Deconjugation

Upon exposure of free thiols on both heavy chain and light chains following deconjugation, resultant secondary reaction products included cysteine and GSH adducts as well as newly reformed disulfide bonds between spatially close free thiols (**Figure 4**). This observation is supported with observed intact mass, and further confirmed with the MS<sup>2</sup> fragmentation for selected parent ions from bottom-up LC-HRMS data (**Figures S5-S7**). The quantification of these secondary, minor, biotransformation species is displayed in **Figure 4**. Furthermore, the deconjugated small molecule linker-payload has been observed to covalently conjugate to circulating albumin (**Table 1**, index 41). The albumin-linker-payload can then also undergo thio-succinimide ring hydrolysis (**Table 1**, index 42).

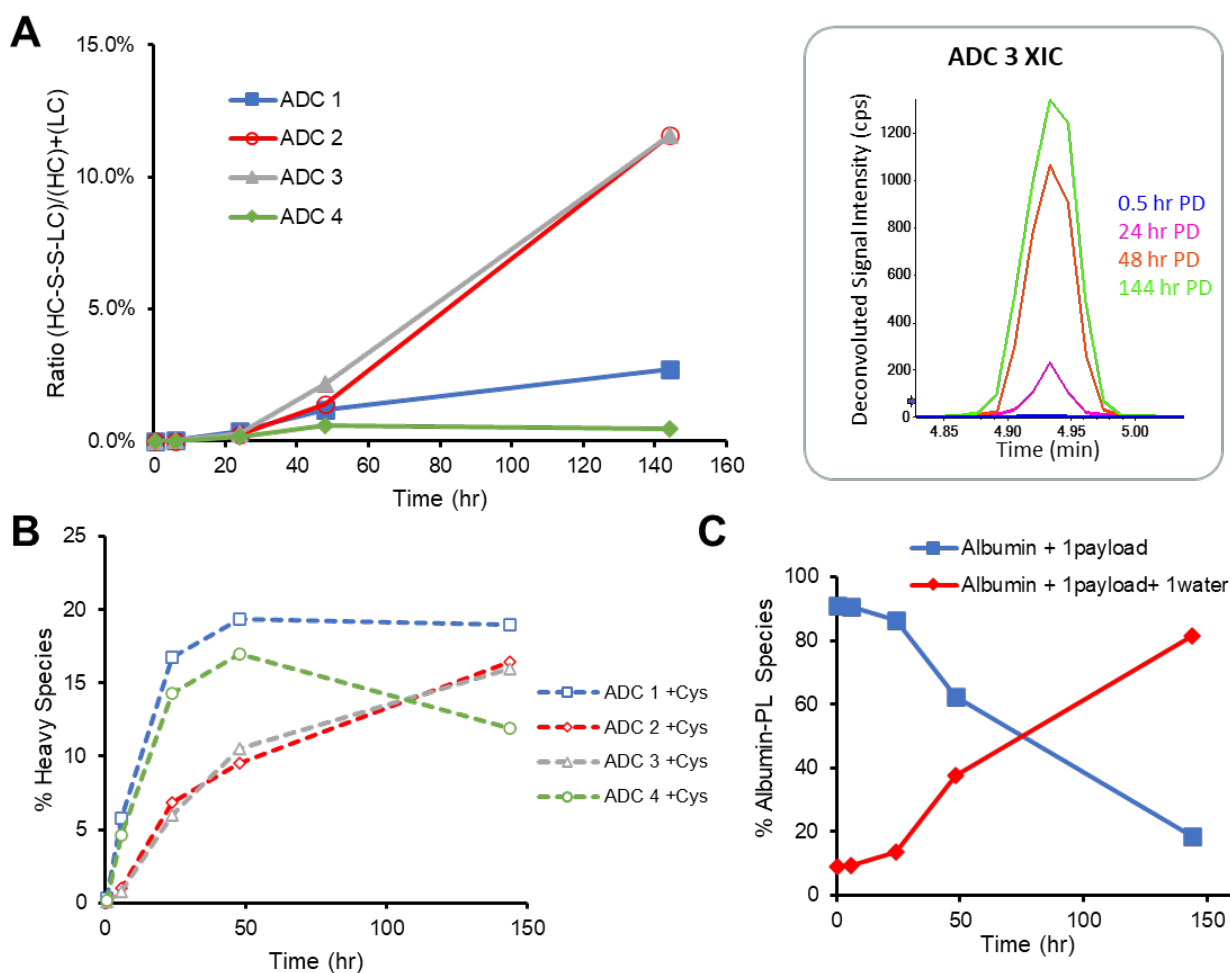


**Figure 4.** Secondary minor biotransformation reactions after linker-payload deconjugation. (A) Formation of the HC-LC inter chain disulfide bond increases with time, the inset figure showed the extracted ion chromatograph for ADC 3 at various timepoints. PD=post dose. (B) Cysteinylation changes over time. (C) Quantification of the thio-succinimide hydrolysis of albumin-linker payload. Representative MS1 spectra can be found in **Figure S5** and **S7**.

It is notable that the HC biotransformation species showed a distinct pattern when comparing the loss of one linker-payload versus the loss of two linker-payloads. After deconjugation of a single linker-payload, we observed a cluster of peaks with several mass changes (**Figure S10C**, **Table 1**, index 11-24), which are indicative of multiple species formed after the exposed free thiol subsequently reacted with other redox-active molecules in plasma. The observed intact mass matched with the proposed adducts and the structure was further confirmed with CID MS<sup>2</sup> spectra (**Figure S5**). On the contrary, after deconjugation of two linker-payloads, the major observed biotransformed species (**Table 1**, index 7-10) had a mass change consistent with the loss of two linker-payloads (e.g. -2296 Da for AZD8205). No additional secondary adducts were observed. The potential reason of the distinct pattern after two payload loss is the reformation of the intra-chain disulfide bond. In the case of the HC-1PL species containing two free exposed thiols and if these thiols are spatially close, reformation of the intra chain disulfide bond becomes the major step 2 reaction. The heavy chain intra-chain disulfide bond was confirmed with bottom-up LC-HRMS with fragmentation (**Figure S6**).

Alternatively, the re-formation of disulfide bonds can happen between the light chain and the heavy chain, following payload deconjugation on both chains. This can be confirmed with the increasing amount of a 76 kDa biotransformation species observed at the 4.9 min retention time (**Figure 4A**, **Figure S10A**). The observed mass matched with the expected mass of light chain and heavy chain conjugated complex, with two linker-payloads remaining on the heavy chain and potential thio-succinimide ring hydrolysis. This inter-chain disulfide bond between light chain-heavy chain was confirmed with bottom-up LC-HRMS with fragmentation (**Figure S7**). For ADCs that deconjugated to greater extent (ADC2 and ADC3), the potential of reformation of the interchain disulfide bond *in vivo* may have contributed to stabilization of the protein scaffold (**Figure 3A**, **4A**, **Table S2**). Interchain disulfide bond reformation was observed for all 4 ADCs, although higher for ADC 2 and 3 (**Figure 4A**). This is likely due to the larger degree of deconjugation, catalyzing the re-formation of the disulfide bonds. After deconjugation, the deconjugated linker-payload can re-conjugate to various thiol-containing endogenous proteins<sup>12</sup>. Capture with anti-payload antibody enables detection and characterization of additional proteins that would contain the re-conjugated linker-payload, such as albumin. Interestingly, albumin conjugated linker-payload continued to hydrolyze over time (**Figure 4B**). These data are consistent with the hypothesis that the linker hydrolysis needs sufficient time for the reaction to proceed and the slower elimination half-life of albumin conjugated linker-payload enables this reaction to be observed on non-antibody containing macromolecular species. Further relative quantification analyses were also performed on the data set. The analysis suggested that glycoforms on the heavy chain do not seem to have a significant impact on the biotransformation at the conjugation site (**Figure S11**). Cysteinylation is the major secondary reaction for the exposed free thiol after deconjugation and also gradually increased over time (**Figure 4C**).

## Thio-succinimide-Conjugated Topoisomerase I inhibitor ADCs Biotransformation Pathways

Consolidating the information comprised of the observed biotransformation species proposed structures, their concentration-time profiles and common chemical reactions that can be expected under such circumstances, we propose the biotransformation pathways for ADC1-4 depicted in **Figure 5**. After dosing, the ADC can undergo two competing reactions: 1) hydrolysis on the thio-succinimide linker,

further stabilizing the conjugated payload and 2) deconjugation of the linker-payload, exposing the free thiol. For AZD8205, the vast majority of ADC went through reaction 1 as the main biotransformation pathway ensuring its *in vivo* stability. Upon deconjugation, further minor biotransformation products were identified. This represents a very small, albeit analytically interesting fraction of the circulating ADC pool.

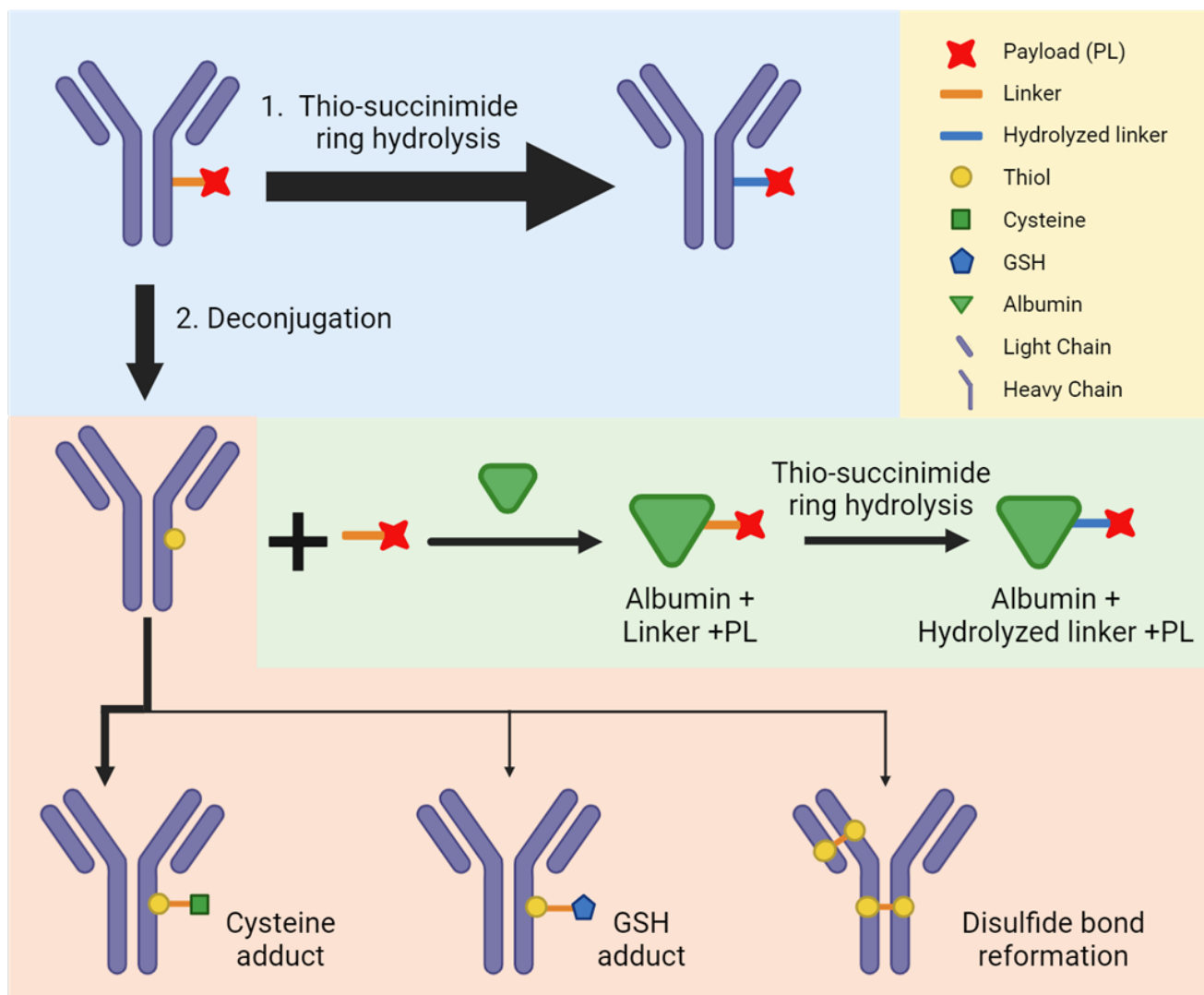


**Figure 5.** Biotransformation pathway diagram for the 4 ADC studied here. Blue box highlights the first step of biotransformation pathway, where the linker thio-succinimide ring is either hydrolyzed, stabilizing the conjugation or deconjugated, exposing the free thiol. Following deconjugation the various components of the ADC can then each go through additional biotransformation reactions. Arrow thickness indicates preponderance of biotransformation pathways. While all ADCs had average DAR ~8, only one linker-payload per ADC is depicted here for simplicity. Created with BioRender.com.

## Discussion

Understanding the underlying mechanisms behind the ADC biotransformation is critical to advance the drug candidate through discovery and development<sup>25</sup>. While for small molecule drug candidates, the ADME studies and metabolite ID analysis is routinely performed, the biotransformation of therapeutic proteins is technically highly challenging. Nonetheless, there is an urgent need for understanding the comprehensive biotransformation profile of therapeutic proteins, because of the rapidly increasing diversity of complex therapeutic protein formats, and the resulting knowledge gap in connecting SAR to drug efficacy and safety.

Biotransformation assessments for therapeutic proteins to-date have largely focused on characterizing amino acid post-translational modifications (PTMs) located in critical regions, proteolytic degradation and glycation or glycosylation<sup>256</sup>. For ADCs, linker/payload stability is often the focus of biotransformation characterization<sup>14, 17, 18</sup>. Payload chemical modification such as deacetylation, adduct formation and partial cleavage have been reported. However, the existing gaps in our understanding of ADC SAR make it essential to further elucidate ADC biotransformation profile of the three critical components determining ADC SAR: the protein scaffold, the conjugation site, and the conjugated payload.

For ADCs, SAR depends not only on the binding properties of the CDRs, but also heavily related to the characteristics of the conjugation site and chemistry, linker, and payload<sup>27-29</sup>. The comprehensive profiling of AZD8205 biotransformations demonstrated that the critical structural determinant contributing to the design of this ADC was the linker structure that either contained propionyl-PEG8 or caproyl spacers. The linker containing the propionyl-PEG8 spacer resulted in increased thio-succinimide hydrolysis rate (**Figure 3A**). While this resulted also in initial increase in deconjugation rate, after approximately 72 hours post-dose the deconjugation rate was reduced by the competing thio-succinimide hydrolysis reaction allowing ADC1 (AZD8205) and ADC4 to effectively maintain a high DAR ratio throughout the dosing period (**Figures 3B and S9B**). Thus, quantitative biotransformation profiling across time can be an informative tool to assess the impact of various structural components on the ADC *in vivo* stability.

Furthermore, LC-HRMS proved to be able to discriminate more readily between subtle changes in DAR compared to the LC-MRM approach as shown in **Figure S9**. We hypothesize that the *direct* DAR analysis using HRMS is more sensitive than the MRM approach which relies on enzymatically released payload as surrogate analyte and measures average DAR indirectly. Importantly, both approaches showed that AZD8205 remained very stable *in vivo*.

Building upon our comprehensive characterization of AZD8205 biotransformation we can glean the various biochemical reactions that enable us to obtain more mechanistic understanding of ADC biotransformation pathways. This is particularly important from translational ADME point of view, as such knowledge would be important to understand the translatability of PK and PD data between animal models and the clinical setting. In addition to the known role of proteases in protein degradation, other endogenous molecules and microenvironments may influence ADC biotransformation. One avenue for interrogating the mechanisms of ADC biotransformation is by examining the endogenous molecules covalently and non-covalently associated with ADCs or their catabolites. Redox pairs such as cysteine and GSH have been observed to interact with AZD8205 and its catabolites. Further understanding of the determinants behind these interactions may provide further supporting evidence in translating these preclinical study results to patients.

Understanding drug metabolism is a critical component for successful drug development<sup>5</sup>. Complex macromolecules such as ADCs present unique challenges to gain such understanding. Therefore, we developed and employed several analytical approaches to profile ADC biotransformation in circulation comprehensively. The results help to better understand factors affecting the underlying pharmacokinetic profiles of the various molecular species which are formed when AZD8205 is administered *in vivo*, and thereby aid in developing better understanding of SAR for thio-succinimide-linked ADCs. In the future, these findings could better inform translation of PK/PD from animal models to the clinical setting. Biotransformation profiling of protein conjugates can be further studied in patient populations, or in specific organ/tissue with this or similar method.

## Conclusion

We have presented a comprehensive profiling approach focused on the *in vivo* biotransformation pathway for a series cysteine-conjugated of ADCs with differing linkers. We employed immuno-affinity capture enrichment, coupled with LC-HRMS and complemented with LC-MRM confirmation, to obtain characterization data at protein subunit level. The HRMS data were interpreted with an unbiased deconvolution method. Key biotransformation species were identified with intact mass and fragmentation approaches, and relative quantification was performed based on the peak area. The elimination of the parent molecule and generation of the biotransformed species as function of time post-dose was used to map the biotransformation reaction pathway of the ADC molecules. When applying this methodology in concert, to a group of ADCs, the structure-stability relationship was established substantiating the importance of the linker structure for this ADC conjugation approach. These data, along with additional information, reported elsewhere<sup>21</sup> led to the selection AZ14170133 as the optimal linker-payload resulting in AZD8205 ADC. To expand our future understanding of bioconjugate and catabolites interactions with endogenous molecules, we will need to apply this methodology, across bioconjugates with varying conjugation approaches, linkers and payloads. Notably, it will also be important to evaluate biotransformation pathways in various microenvironments either in specific organs/tissues or tumors to fully understand the determinants for their efficacy/safety profile. Eventually, the biotransformation information obtained in animal models/*in vitro* experiments may be translated to potential patient populations as part of clinical studies.

### Acknowledgment:

Y.H., H.Y.T., J. Yuan, R.M., J. Yang, K.B., B.V., L.M., K.K., N.L., M.L., and A.I.R. are or were employees of AstraZeneca at the time this work was conducted and may hold stock ownership and/or stock options or interests in the company. This study was funded by AstraZeneca.

## References

1. Petrotchenko, E. V.; Borchers, C. H., Protein Chemistry Combined with Mass Spectrometry for Protein Structure Determination. *Chem Rev* **2022**, 122 (8), 7488-7499.
2. Mielke, S. P.; Krishnan, V. V., Characterization of protein secondary structure from NMR chemical shifts. *Prog Nucl Magn Reson Spectrosc* **2009**, 54 (3-4), 141-165.
3. Chen, B.; Peng, Y.; Valeja, S. G.; Xiu, L.; Alpert, A. J.; Ge, Y., Online Hydrophobic Interaction Chromatography-Mass Spectrometry for Top-Down Proteomics. *Anal Chem* **2016**, 88 (3), 1885-91.

4. Skinner, O. S.; Haverland, N. A.; Fornelli, L.; Melani, R. D.; Do Vale, L. H. F.; Seckler, H. S.; Doubleday, P. F.; Schachner, L. F.; Szentic, K.; Kelleher, N. L.; Compton, P. D., Top-down characterization of endogenous protein complexes with native proteomics. *Nat Chem Biol* **2018**, *14* (1), 36-41.
5. Schadt, S.; Hauri, S.; Lopes, F.; Edelmann, M. R.; Staack, R. F.; Villasenor, R.; Kettenberger, H.; Roth, A. B.; Schuler, F.; Richter, W. F.; Funk, C., Are Biotransformation Studies of Therapeutic Proteins Needed? Scientific Considerations and Technical Challenges. *Drug Metab Dispos* **2019**, *47* (12), 1443-1456.
6. Mu, R.; Yuan, J.; Huang, Y.; Meissen, J. K.; Mou, S.; Liang, M.; Rosenbaum, A. I., Bioanalytical Methods and Strategic Perspectives Addressing the Rising Complexity of Novel Bioconjugates and Delivery Routes for Biotherapeutics. *BioDrugs* **2022**, *36* (2), 181-196.
7. Hall, M. P., Biotransformation and in vivo stability of protein biotherapeutics: impact on candidate selection and pharmacokinetic profiling. *Drug Metab Dispos* **2014**, *42* (11), 1873-80.
8. Szijj, P. A.; Bahou, C.; Chudasama, V., Minireview: Addressing the retro-Michael instability of maleimide bioconjugates. *Drug Discov Today Technol* **2018**, *30*, 27-34.
9. Huang, Y.; Mou, S.; Wang, Y.; Mu, R.; Liang, M.; Rosenbaum, A. I., Characterization of Antibody-Drug Conjugate Pharmacokinetics and in Vivo Biotransformation Using Quantitative Intact LC-HRMS and Surrogate Analyte LC-MRM. *Anal Chem* **2021**, *93* (15), 6135-6144.
10. Hyung, S. J.; Leipold, D. D.; Lee, D. W.; Kaur, S.; Saad, O. M., Multiplexed Quantitative Analysis of Antibody-Drug Conjugates with Labile CBI-Dimer Payloads In Vivo Using Immunoaffinity LC-MS/MS. *Anal Chem* **2022**, *94* (2), 1158-1168.
11. Joubert, N.; Beck, A.; Dumontet, C.; Denevault-Sabourin, C., Antibody-Drug Conjugates: The Last Decade. *Pharmaceuticals (Basel)* **2020**, *13* (9).
12. Zhao, P.; Zhang, Y.; Li, W.; Jeanty, C.; Xiang, G.; Dong, Y., Recent advances of antibody drug conjugates for clinical applications. *Acta Pharm Sin B* **2020**, *10* (9), 1589-1600.
13. Hafeez, U.; Parakh, S.; Gan, H. K.; Scott, A. M., Antibody-Drug Conjugates for Cancer Therapy. *Molecules* **2020**, *25* (20).
14. Su, D.; Zhang, D., Linker Design Impacts Antibody-Drug Conjugate Pharmacokinetics and Efficacy via Modulating the Stability and Payload Release Efficiency. *Front Pharmacol* **2021**, *12*, 687926.
15. Shen, B. Q.; Xu, K.; Liu, L.; Raab, H.; Bhakta, S.; Kenrick, M.; Parsons-Reponte, K. L.; Tien, J.; Yu, S. F.; Mai, E.; Li, D.; Tibbitts, J.; Baudys, J.; Saad, O. M.; Scales, S. J.; McDonald, P. J.; Hass, P. E.; Eigenbrot, C.; Nguyen, T.; Solis, W. A.; Fuji, R. N.; Flagella, K. M.; Patel, D.; Spencer, S. D.; Khawli, L. A.; Ebens, A.; Wong, W. L.; Vandlen, R.; Kaur, S.; Sliwkowski, M. X.; Scheller, R. H.; Polakis, P.; Junutula, J. R., Conjugation site modulates the in vivo stability and therapeutic activity of antibody-drug conjugates. *Nat Biotechnol* **2012**, *30* (2), 184-9.
16. Zhu, X.; Huo, S.; Xue, C.; An, B.; Qu, J., Current LC-MS-based strategies for characterization and quantification of antibody-drug conjugates. *J Pharm Anal* **2020**, *10* (3), 209-220.
17. He, J.; Su, D.; Ng, C.; Liu, L.; Yu, S. F.; Pillow, T. H.; Del Rosario, G.; Darwish, M.; Lee, B. C.; Ohri, R.; Zhou, H.; Wang, X.; Lu, J.; Kaur, S.; Xu, K., High-Resolution Accurate-Mass Mass Spectrometry Enabling In-Depth Characterization of in Vivo Biotransformations for Intact Antibody-Drug Conjugates. *Anal Chem* **2017**, *89* (10), 5476-5483.
18. He, J.; Yu, S. F.; Yee, S.; Kaur, S.; Xu, K., Characterization of in vivo biotransformations for trastuzumab emtansine by high-resolution accurate-mass mass spectrometry. *MAbs* **2018**, *10* (7), 960-967.
19. Su, D.; Chen, J.; Cosino, E.; Dela Cruz-Chuh, J.; Davis, H.; Del Rosario, G.; Figueroa, I.; Goon, L.; He, J.; Kamath, A. V.; Kaur, S.; Kozak, K. R.; Lau, J.; Lee, D.; Lee, M. V.; Leipold, D.; Liu, L.; Liu, P.; Lu, G. L.; Nelson, C.; Ng, C.; Pillow, T. H.; Polakis, P.; Polson, A. G.; Rowntree, R. K.; Saad, O.; Safina, B.; Stagg, N. J.; Tercel, M.; Vandlen, R.; Vollmar, B. S.; Wai, J.; Wang, T.; Wei, B.; Xu, K.; Xue, J.; Xu, Z.; Yan, G.; Yao, H.; Yu, S. F.; Zhang, D.; Zhong, F.; Dragovich, P. S., Antibody-Drug Conjugates Derived from

Cytotoxic seco-CBI-Dimer Payloads Are Highly Efficacious in Xenograft Models and Form Protein Adducts In Vivo. *Bioconjug Chem* **2019**, *30* (5), 1356-1370.

20. Kotapati, S.; Passmore, D.; Yamazoe, S.; Sanku, R. K. K.; Cong, Q.; Poudel, Y. B.; Chowdari, N. S.; Gangwar, S.; Rao, C.; Rangan, V. S.; Cardarelli, P. M.; Deshpande, S.; Strop, P.; Dollinger, G.; Rajpal, A., Universal Affinity Capture Liquid Chromatography-Mass Spectrometry Assay for Evaluation of Biotransformation of Site-Specific Antibody Drug Conjugates in Preclinical Studies. *Anal Chem* **2020**, *92* (2), 2065-2073.

21. Kinneer, K.; Wortmann, P.; Cooper, Z. A.; Dickinson, N. J.; Masterson, L.; Cailleau, T.; Hutchinson, I.; Vijayakrishnan, B.; McFarlane, M.; Ball, K.; Davies, M.; Lewis, A.; Huang, Y.; Rosenbaum, A. I.; Yuan, J.; Chesebrough, J.; Anderton, J.; Monks, N.; Novick, S.; Wang, J.; Dimasi, N.; Christie, R. J.; Sabol, D.; Tosto, F. A.; Wallez, Y.; Leo, E.; Albertella, M. R.; Staniszewska, A. D.; Tice, D. A.; Howard, P. W.; Luheshi, N.; Sapra, P., Design and Preclinical Evaluation of a Novel B7-H4-Directed Antibody-Drug Conjugate, AZD8205, Alone and in Combination with the PARP1-Selective Inhibitor AZD5305. *Clin Cancer Res* **2022**.

22. Kinneer, K.; Dickinson, N. J.; Masterson, L.; Cailleau, T.; Hutchinson, I.; Vijayakrishnan, B.; Dimasi, N.; Christie, R. J.; McFarlane, M.; Ball, K.; Lewis, A.; Koch, S.; Brown, L.; Huang, Y.; Rosenbaum, A. I.; Yuan, J.; Mou, S.; Monks, N. R.; Chesebrough, J.; Tammali, R.; Anderton, J.; Sabol, D.; Tosto, F. A.; Wortmann, P.; Cooper, Z. A.; Ryan, P.; Hood, J.; Teruel, C. F.; Traynor, C. S.; Pike, A.; Davies, M.; Leo, E.; Cook, K.; Luheshi, N.; Howard, P. W.; Sapra, P., Abstract 1765: Discovery and first disclosure of AZD8205, a B7-H4-targeted antibody-drug conjugate utilizing a novel topoisomerase I linker-warhead. *Cancer Research* **2022**, *82* (12\_Supplement), 1765-1765.

23. Meric-Bernstam, F.; Oh, D.-Y.; Naito, Y.; Shimizu, T.; Chung, V.; Park, H.; Gaillard, S.; Wang, F.; Cooper, Z. A.; Kinneer, K.; Rebelatto, M.; Kirby, L.; Luheshi, N.; Miller, N.; Varga, A.; Mileschkin, L. R., First-in-human study of the B7-H4 antibody-drug conjugate (ADC) AZD8205 in patients with advanced/metastatic solid tumors. **2022**, *40* (16\_suppl), TPS3153-TPS3153.

24. Huang, Y.; Del Nagro, C. J.; Balic, K.; Mylott, W. R., Jr.; Ismaiel, O. A.; Ma, E.; Faria, M.; Wheeler, A. M.; Yuan, M.; Waldron, M. P.; Peay, M. G.; Cortes, D. F.; Roskos, L.; Liang, M.; Rosenbaum, A. I., Multifaceted Bioanalytical Methods for the Comprehensive Pharmacokinetic and Catabolic Assessment of MEDI3726, an Anti-Prostate-Specific Membrane Antigen Pyrrolbenzodiazepine Antibody-Drug Conjugate. *Anal Chem* **2020**, *92* (16), 11135-11144.

25. Kellie, J. F.; Pannullo, K. E.; Li, Y.; Fraley, K.; Mayer, A.; Sychterz, C. J.; Szapacs, M. E.; Karlinsey, M. Z., Antibody Subunit LC-MS Analysis for Pharmacokinetic and Biotransformation Determination from In-Life Studies for Complex Biotherapeutics. *Anal Chem* **2020**, *92* (12), 8268-8277.

For Table of Contents Only

